JOINT BAYESIAN DETECTION OF BRAIN ACTIVATED REGIONS AND LOCAL HRF ESTIMATION IN FUNCTIONAL MRI

David Afonso João Sanches Martin H. Lauterbach (MD)

Institute for Systems and Robotics, Instituto Superior Técnico, Lisbon, Portugal
Faculty of Medicine, University of Lisbon, Portugal

ABSTRACT

The blood-oxygenation-level-dependent (BOLD) signal, measured with the *Magnetic Resonance Imaging* (MRI), is currently used to detect the activation of brain regions with a stimulus application, e.g., visual or auditive. In a block design approach, the stimuli (called *paradigm* in the *fMRI* scope) are designed to detect activated and non activated brain regions with maximized certainty. However, corrupting noise in MRI volumes acquisition, patient motion and the normal brain activity interference makes this detection a difficult task.

In this paper a new Bayesian method, called *SPM-MAP*, is proposed where a joint detection of brain activated regions and estimation of the underlying *hemodynamic impulse response function* (HRF) is proposed.

Monte Carlo tests on its error probability and HRF estimation with synthetic data are performed and presented.

Index Terms— Functional MRI, Activity Detection, Bayesian

I. INTRODUCTION

Functional Magnetic Resonance Imaging (fMRI) is the most prominent method used to detect brain activated regions involved in particular tasks. This modality relies on changes in blood oxygenation and volume, consequence of the hemodynamic response events related to local neural activity. This signal, called blood-oxygenation-level-dependent (BOLD), results from the endogenous magnetic contrast between 0xyhaemoglobin (diamagnetic) and deoxyhaemoglobin (paramagnetic). Hence, increased blood volume reduces the local concentration of deoxygenated hemoglobin causing an increase in the magnetic resonance (MR) signal on a T2 or T2*-weighted image [1].

The goal is the visualization of the statistical map representation of which areas are activated after the stimulatus paradigm application during the scan. To obtain the desirable results, several processing steps are usually involved, e.g. image preprocessing (motion and noise correction), spacial normalization transformation, statistical tests and the final inferences procedures [2]. Considering the last two steps, which are the focus of this paper, the general approach is to express the observed response variable in terms of a linear combination of explanatory variables (EVs) [3] (which include a rigid HRF estimate), and makes use of classical statistics (T or F tests) to infer activity, using e.g. a p-value threshold.

Correspondent author: D. Afonso (dafonso@isr.ist.utl.pt). This work was supported by Fundação para a Ciência e a Tecnologia (ISR/IST plurianual funding) through the POS Conhecimento Program which includes FEDER funds. This work was done in partial collaboration with Hospital da Cruz Vermelha de Lisboa. An acknowledgment to Henrik Halvorsen for revision

The inference results are strongly dependent on the HRF estimation, which is usually not known. In the literature there are two different approaches for the HRF modeling. The most common approach is purely heuristic, using known functions (e.g. gamma functions [2], or Gaussian functions to fit the experimental data. The second approach is physiological, modeling the underlying physiological process involved in the BOLD signal generation, e.g. the Balloon Model [4] which is often used and augmented.

In this paper a time invariant linear *infinite impulse response* (IIR) model is used, called *physiologically based hemodynamic* (PBH) model [5], which is simplicity and physiologically sound.

This paper proposes a new algorithm that jointly detects the brain activity (which leads to a functional brain map) and the local HRF estimation, in order to minimize the detection error probability.

In order to estimate the binary (activated or not) information on each voxel (volume element), a Bayesian approach is used to force a binary solution for the EV's and the corresponding optimal HRF estimating.

Monte Carlo tests are performed using synthetic data, where the activity detection errors probability and the mean HRF estimations are presented for several amounts of corrputing.

The rest of the paper is organized as follows. Section II formulates the problem and In Section III the estimation Bayesian method is presented. Section IV presents the experimental results and section V concludes the paper.

II. PROBLEM FORMULATION

Each voxel, after the application of a given paradigm (a combination of stimulus time-courses) may be activated by one or more applied stimulus ($\exists_k : \beta_k = 1$) or may not be activated at all ($\forall_k : \beta_k = 0$).

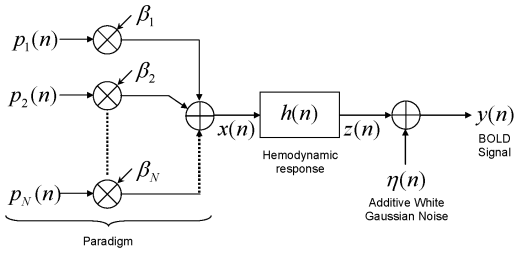

Fig. 1. BOLD signal generation model.

The signal BOLD associated with each voxel along the time (*time course*) is dealt in a 1D basis, independently of the other voxels. The data observation model, displayed in Fig. 1, is the following

$$y(n) = h(n) * \sum_{k=1}^{N} \beta_k p_k(n) + \eta(n) \quad (1)$$

where $\eta(n)$ is *additive white Gaussian noise* (AWGN), $h(n)$ is the hemodynamic response function of the brain tissues, $p_k(n)$ are the stimulus signals along time and β_k are unknown binary variables to model the activation of the voxel by the k[th] stimulus.

The *Statistical Parametric Mapping* algorithm (SPM) proposed here, designed in a Bayesian framework and using the *maximum a posteriori* (MAP) criterion is called *SPM-MAP*[1]. It jointly estimates the vector $\mathbf{b} = \{\beta_1, \beta_2, ..., \beta_N\}^T$, associated with each voxel and the corresponding hemodynamic response, $h(n)$, which can be denoted in vectorial form, $\mathbf{h} = \{h(1), h(2), ..., h(L)\}^T$, where L is the number of $\mathbf{y}$ observations.

The physiologicaly based HRF model [5] used in this paper has the following third order discrete transfer function

$$H(z) = \frac{b_0 + b_1 z^{-1} + b_2 z^{-2}}{1 + a_1 z^{-1} + a_2 z^{-2} + a_3 z^{-3}} \tag{2}$$

where the coefficients b_k and a_k must be estimated.

The estimation process is performed by minimizing an energy function depending on the binary unknowns β_k, on the hemodynamic response $h(n)$ and on the observations $y(n)$ (see Fig. 1). The direct estimation of the $H(z)$ coefficients is a difficult task because it is not easy to define simple priors for these coefficients based on the desired time response $h(n)$. Therefore, to overcome this difficulty, instead of estimating the a_k and b_k IIR coefficients, a FIR is estimated, $\mathbf{g} = \{g(1), g(2), ..., g(F)\}^T$, with length $F \leq L$. In each iteration this estimated response is projected into the $H(z)$ space, i.e., the set of coefficients a_k and b_k are estimated in order to minimize $\|g(n) - h(n)\|$. The first F samples of $h(n)$ are used to obtain a new estimate of the binary unknowns β_k. This process is repeated until convergence is achieved.

The signal $\mathbf{x} = \{x(1), x(2), x(3), ..., x(L)\}^T$ (see Fig. 1) may be expressed as $\mathbf{x} = \theta\mathbf{b}$ where

$$\theta = \begin{pmatrix} p_1(1) & p_2(1) & p_3(1) & ... & p_N(1) \\ p_1(2) & p_2(2) & p_3(2) & ... & p_N(2) \\ p_1(3) & p_2(3) & p_3(3) & ... & p_N(3) \\ \vdots & \vdots & \vdots & ... & \vdots \\ p_1(L) & p_2(L) & p_3(l) & ... & p_N(L) \end{pmatrix} \tag{3}$$

.

The output vector of $H(z)$, displayed in Fig. 1, $\mathbf{z} = \{z(1), z(2), z(3), ...z(L)\}^T$, is obtained by convolving $\mathbf{h}$ with $\mathbf{x}$, $z(n) = h_F(n) * x(n)$, where $h_F(n)$ are the first F samples of $h(n)$. The output signal may be expressed in the two following ways i) $\mathbf{z} = H\mathbf{x}$ and ii) $\mathbf{z} = \Phi\mathbf{h}$ where H and Φ are the following $L \times L$ and $L \times p$ Toeplitz matrices respectively

$$H = \begin{pmatrix} h(1) & 0 & 0 & 0 & 0 & 0 \\ h(2) & h(1) & 0 & 0 & 0 & 0 \\ h(3) & h(2) & h(1) & 0 & 0 & 0 \\ \vdots & \vdots & \vdots & \vdots & \vdots & \vdots \\ 0 & ... & h(p) & h(p-1) & ... & h(1) \end{pmatrix} \tag{4}$$

$$\Phi = \begin{pmatrix} x(1) & 0 & 0 & 0 & 0 \\ x(2) & x(1) & 0 & 0 & 0 \\ \vdots & \vdots & \vdots & \vdots & 0 \\ x(L) & x(L-1) & ... & ... & x(L-P+1) \end{pmatrix} \tag{5}$$

[1]*Statistical parametric mapping is generally used to identify functionally specialized brain responses*[3]

The observed BOLD signal $y(n)$, $\mathbf{y} = \{y(1), y(2), ..., y(L)\}^T$ can therefore be obtained with the following two ways

$$\mathbf{y} = \Psi\mathbf{b} + \mathbf{n} \tag{6}$$

$$\mathbf{y} = \Phi\mathbf{h} + \mathbf{n} \tag{7}$$

where $\Psi = H\theta$ and $\mathbf{n} = \{\eta(1), \eta(2), ..., \eta(L)\}^T$ is a vector of *independent and identically distributed* (i.i.d) zero mean random variables normally distributed, that is, $p(\eta(k)) = N(0, \sigma_y^2)$. This additive white gaussian noise (AWGN) is usually used to model the corruption process in functional MRI, although other models may also be used, e.g., *Rice* and *Rayleigh* distributions. In this work we suppose that the motion correction preprocessing step was efficient enough to remove most of the temporal correlation between voxels, and so its influence is included and corrected along with the corruption noise.

III. ESTIMATION

The *maximum a posteriori* (MAP) estimation is obtained by minimizing the following energy function

$$E(y, \mathbf{x}(\mathbf{b}), \mathbf{h}) = E_y(\mathbf{y}, \mathbf{x}(\mathbf{b}), \mathbf{h}) + E_b(\mathbf{b}) + E_h(\mathbf{x}(\mathbf{b})) \tag{8}$$

where the *data fidelity term* $E_y(\mathbf{y}, \mathbf{x}(\mathbf{b}), \mathbf{h}) = -\log(p(\mathbf{y}|\mathbf{x}(\mathbf{b})))$ and the prior terms associated to the unknowns to be estimated, $\mathbf{b} = \{\beta_1, ...\beta_N\}$ and $\mathbf{h} = \{h(0), ..., h(p-1)\}$ are $E_b(\mathbf{b}) = -\log(p(\mathbf{b}))$ and $E_h(\mathbf{x}(\mathbf{b})) = -\log(p(\mathbf{h}))$ respectively. These priors incorporate the *a priori* knowledge about the unknowns to be estimated, that is, β_k are binary and $h(n)$ is smooth.

The estimation process is performed in the following sequential three steps,

$$\mathbf{b}^t = \arg\min_{\beta} E(\mathbf{y}, \mathbf{x}(\mathbf{b}^{t-1}), \mathbf{h}^{t-1}) \tag{9}$$

$$\mathbf{g} = \arg\min_{h} E(\mathbf{y}, \mathbf{x}(\mathbf{b}^t), \mathbf{h}^{t-1}) \tag{10}$$

$$\mathbf{h}^t = \text{Proj}_{FIR}\left[\text{Proj}_{IIR}(\mathbf{g})\right] \tag{11}$$

where $()^t$ means estimation at t^{th} iteration and $Proj$ stands for the projection operation by using the *minimum square error* (MSE) criterion. The Proj_{IIR} problem is not trivial [6]. In this paper the approximation algorithm proposed by *Shanks* [6] is used.

The assumption of statistical independence for the observations means that $p(\mathbf{y}|\mathbf{x}(\mathbf{b}), \mathbf{h}) = \prod_{i=1}^{L} p(y(i)|(x * h)(i))$ where $p(y_i) \sim \mathcal{N}((x * h)(i), \sigma_y^2)$. The parameters β_k to be estimated are also assumed independent, that is, $p(\mathbf{b}) = \prod_{i=1}^{N} p(\beta_k)$ where $p(\beta_k)$ is a bi-modal distribution defined as a sum of two Gaussian distributions centered at zero and one, with ${\sigma_\beta}^2$ variance.

$$p(\beta_k) = \frac{1}{2}\left[N(0, \sigma_\beta^2) + N(1, \sigma_\beta^2)\right] \tag{12}$$

because β_k are assumed to be binary variables, $\beta_k \in \{0, 1\}$. In order to better approximate the binary answer, the σ_β parameter should be as small as possible but numerical stability reasons prevent the adoption of too small values. The prior term $E_b(b)$ may therefore be written as

$$E_b(\mathbf{b}) = \sum_{k=1}^{N}\left[\frac{2\beta_k^2 - 2\beta_k + 1}{4\sigma_\beta^2} - \log\left(\cosh\left[\frac{2\beta_k - 1}{4\sigma_\beta^2}\right]\right)\right]. \tag{13}$$

The smoothness of $h(n)$ is obtained by using a Gibbs distribution to model $\mathbf{h}$, $p(\mathbf{h}) = \frac{1}{Z_h} e^{-\alpha \sum_{n=2}^{N} (h(n)-h(n-1))^2}$ which leads to

$$E_{\mathbf{h}}(\mathbf{x}(\mathbf{b})) = -\log(p(\mathbf{h})) = \alpha(\Delta\mathbf{h})^T(\Delta\mathbf{h}) + C \tag{14}$$

where α is a parameter that tunes the smoothing degree for $h(n)$, C is a constant, Z_h is a partition function and Δ is the following difference operator

$$\Delta = \begin{pmatrix} 1 & 0 & 0 & ... & 0 & -1 \\ -1 & 1 & 0 & ... & 0 & 0 \\ 0 & -1 & 1 & ... & 0 & 0 \\ \vdots & \vdots & \vdots & ... & 0 & 0 \\ 0 & 0 & 0 & ... & -1 & 1 \end{pmatrix} \tag{15}$$

The energy function (8) to be minimized, $E(\mathbf{y}, \mathbf{x}(\mathbf{b}), \mathbf{h})$, has the following formats in step one and step two respectively

$$E_1 = \frac{1}{2\sigma_y^2}(\Psi\mathbf{b} - \mathbf{y})^T(\Psi\mathbf{b} - \mathbf{y}) + E_b(\mathbf{b}) + C_1 \tag{16}$$

$$E_2 = \frac{1}{2\sigma_y^2}(\Phi\mathbf{h} - \mathbf{y})^T(\Phi\mathbf{h} - \mathbf{y}) + \alpha\mathbf{h}^T(\Delta^T\Delta)\mathbf{h} + C_2. \tag{17}$$

The MAP estimate is obtained by finding the $E(\mathbf{y}, \mathbf{x}(\mathbf{b}), \mathbf{h})$ stationary point, $\nabla E(\mathbf{y}, \mathbf{x}(\mathbf{b}), \mathbf{h}) = 0$ where (∇) is the gradient operator.

In the first step $\mathbf{b}$ is estimated by solving the following equation

$$\nabla_b E_1 = \Psi^T(\Psi\mathbf{b} - \mathbf{y}) + \frac{\sigma_y^2}{\sigma_\beta^2}\left[\mathbf{b} - \frac{1}{2}R(\mathbf{b})\right] = 0 \tag{18}$$

where ∇_b is the gradient operator with respect to $\mathbf{b}$ and $R(\mathbf{b})$ is a column vector with N elements

$$r_k = 1 + tanh\left[\frac{2\beta_k - 1}{4\sigma_\beta^2}\right] \tag{19}$$

. The solution of (18) is obtained by using the fixed point method which leads to the following recursion

$$\hat{\mathbf{b}}^t = (\Psi^T\Psi + \lambda I)^{-1}(\Psi^T y + \frac{\lambda}{2}R(\hat{\mathbf{b}}^{t-1})) \tag{20}$$

where $\lambda = \sigma_y^2/2\sigma_\beta^2$ is a parameter, I is a N dimensional identity matrix and $\hat{\mathbf{b}}^t$ is the $\mathbf{b}$ estimate at t$^{\text{th}}$ iteration.

In the second step, $h_N(n)$ is estimated by solving the following equation

$$\nabla_h E_2 = \Phi^T(\Phi\mathbf{h} - \mathbf{y}) + 2\lambda\sigma_y^2 L\mathbf{h} = 0 \tag{21}$$

where ∇_h is the gradient operator with respect to $\mathbf{h}$ and $L = \Delta^T\Delta$ (see (15)). The solution of (21) is

$$\mathbf{g} = \left[\Phi^T\Phi + 2\lambda\sigma_y^2 L\right]^{-1}\Phi^T\mathbf{y} \tag{22}$$

where $\Phi(\mathbf{x}(\mathbf{b}))$ is computed with the $\mathbf{b}$ estimate obtained (20) in step one, $\hat{\mathbf{b}}^t$.

Finally $\mathbf{g}$ is projected in the space of the admissible responses of $H(z)$ and afterward re-projected in the FIR space, $\mathbf{h} = \text{Proj}_{FIR}[\text{Proj}_{IIR}(\mathbf{g})]$. This projection step is needed because the HRF smoothness constraints is much more easy to define in the time domain than in the parameters domain of the IIR model. However, this FIR response does not necessarily belong to the responses space of the adopted IIR PBH model, presented in section II. The $\mathbf{g} \rightarrow IIR$ projection is performed by using the *Shanks's* method [6] and then, re-projection in the FIR space is nothing more than computing the L first samples of $h(n)$.

These three steps are repeated until convergence is achieved.

To accomplish the desired binary nature of $\hat{\mathbf{b}}$, the following threshold is applied to $\hat{\beta}_k$

$$\hat{b}_k = \begin{cases} 0 & \hat{\beta}_k < 0.5 \\ 1 & otherwise \end{cases} \tag{23}$$

and these are the activation parameters that provide information on whether the brain area represented in the corresponding voxel was activated by each of the paradigm stimulus or not.

IV. EXPERIMENTAL RESULTS

In this section Monte Carlo tests of the proposed *SPM-MAP* method are presented in order to evaluate the performance of the algorithm. Two synthetic binary images of 128x128 pixels where generated, which represent a single BOLD slice signal, as can be seen overlapped in the Fig. 2 (with the error resultant from the estimation). In it, colored voxels (red, yellow and white) where activated by, at least, a stimulus paradigm and the black pixels where not activated at all. So according to the mathematical notation presented above, red: $\mathbf{b} = \{1, 0\}^T$; yellow: $\mathbf{b} = \{0, 1\}^T$; white: $\mathbf{b} = \{1, 1\}^T$ and black: $\mathbf{b} = \{0, 0\}^T$, which is the activation ground truth to be estimated for each voxel.

The BOLD signal, $y(n)$, is generated by using the model presented in Fig. 1. A reasonable two stimuli block-design paradigm, $p_1(n)$ and $p_2(n)$, of 10 seconds task duration followed by a 30 second rest period each in 5 epochs, were used in order to obtain a non superposition of $p_1(n)$ and $p_2(n)$ while allowing for the BOLD signal to decay to rest. The true impulse HRF signal, $h(n)$, was generated from a representative IIR, selected from the PBH estimation on real single-event data [5], and the following noise energies were used: $\sigma_y = \{0.2, 0.5, 0.7, 0.8, 1\}$. These noise energies are better evaluated when compared against the BOLD signal energy level, which is done with the *signal-to-noise ratio* ($SNR = 10\log\sum_1^N \frac{[(\beta_1 \times p_1(n) + \beta_2 \times p_2(n)) * h(n)]^2}{\sigma_y^2}$) for the two data cases in which the BOLD signal is present: $\sum_{k=1}^{2} \mathbf{b}(k) \geq 1$ (see Table I).

This generated synthetic data is equivalent to $2 \times 128 \times 128 = 32768$ independent $y(n)$ time-courses, containing all possible combinations for the $\mathbf{b}$ vector. These are used on Monte Carlo tests to compute the $P_e(\sigma, N) = \frac{1}{R}\sum_{i=1}^{R}|\hat{b}_i - b_i|$, and the results graphically presented in Fig. 2 and in Table I).

σ_y	0.2	0.5	0.7	0.8	1
$SNR(dB)$	7.3;11	-0.63;2.6	-3.6;-0.37	-4.7;-1.5	-6.7;-3.5
$P_e(\%)$	0.0427	0.0916	0.168	0.260	4.27
$\dot{P}_e(\%)$	0	0	0.0244	0.0245	1.51
$\ddot{P}_e(\%)$	0	0	0.0073	0.0061	0.513

Table I. Monte Carlo P_e (IV) of *SPM-MAP* for several values of AWGN σ_y and correspondent SNR values for the $\sum_{k=1}^{2} \mathbf{b}(k) \geq 1$ two different signal energy situations. Spatial correlation correction is exemplified in $\dot{P}_e$ and $\ddot{P}_e$ where one and two isolated pixels were dismissed, respectively.

Table I shows that even for high noise levels the proposed *SMP-MAP* method presents a $P_e < 0.3\%$. It is important to point-out that although the SNR in MRI depends on a large number of variables, it is usually more than $1dB$ [2]. So the most realistic σ_y values would be situated between 0.2 and 0.5, for the data used. In this

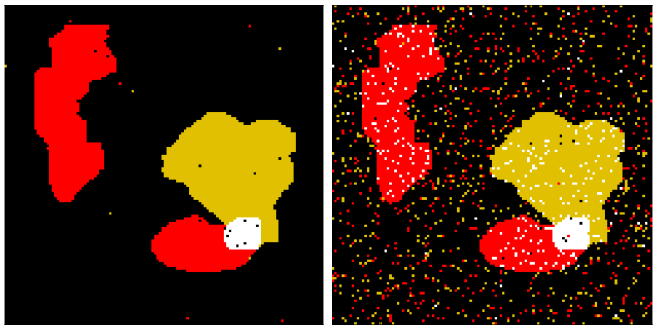

Fig. 2. *SPM-MAP* activation detection results for $\sigma_y = 0.5$ (up) and $\sigma_y = 1$ (down). Brain areas activated by two paradigms (red and yellow), with a functional overlapping region (white) and non activated areas (black).

range, the method achieves values of $P_e < 0.1\%$. Furthermore, for the very high noise amount of $\sigma_y = 1$ ($SNR = [-6.7; -3.5]$) the P_e stays below 5%, resulting in the bottom image in Fig. 2. Notice that when looking at Fig. 2, the intuitive notion on the error probability might seem higher than the refered 0.1% and 0.5% values, due to the fact that the images are actualy a overlap of two images.

It is intuitive when looking at the results in figure 2, that the accuracy of the method can be improved if spacial correlation information is included, removing several of those isolated, spatially uncorrelated, voxels. For illustration purposes, the P_e is recalculated after removing areas of one ($\dot{P}_e$) and two ($\ddot{P}_e$) isolated voxels in an 8 voxels neighborhood. The resultant error probabilities (see Table I) decreases for all the noise amounts, yielding null for the 0.2 and 0.5 σ_y values.

The HRF estimation results are harder to analyze. For each one of the 32768 voxels a $h(n)$ HRF is estimated, but only the ones corresponding to activated brain areas $\beta_k = 1$ are relevant. So, in the false-negative case, that information is discarded. On the other hand, the false-positive case is not discarded and the $h(n)$ tends to follow the random AWGN form, around zero. These last situations reduce the amplitude of the HRF mean, computed over all positive estimated voxels $\hat{\beta}_k$, including false-positives. This effect can be seen in Fig. 3, where the false-positives effect is removed. Considering that in real data we do not have information on false-positives, a correction could be done dismissing estimated $h(n)$ functions with AWGN distribution, but since the primary goal of this work is the activation detection, this is left for further works. Furthermore there is a global decrease in amplitude of every HRF estimation in the $FIR \rightarrow IIR$ projection operation, which can be seen on figure 3 right column. In fact, when there is not an IIR filter that perfectly describes the estimated $g(n)$ FIR, the IIR computed by the Shanks [6,7] algorithm is always of lower amplitude. In spite of all this, the HRF estimation provided reasonable results (Fig. 3) and proved robust even in high noise levels.

V. CONCLUSIONS

In this paper a new Bayesian method is presented, where the neural activity detection is jointly obtained along with the HRF estimation. This approach presents two main advantages: *1)* the activity detection benefits from iterative and adaptative nature of the HRF shape estimation; *2)* it provides local, space variant, HRF

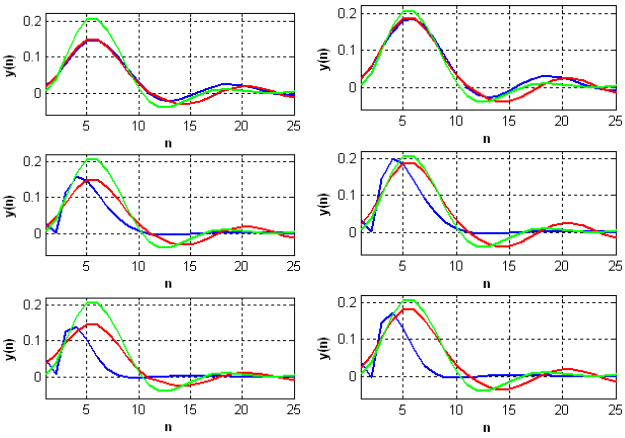

Fig. 3. Mean HRF estimation results considering all $\hat{\beta}_k \neq 0$ estimations (left) and for only the $\hat{b}_k \neq 0$ correct ones (right), for $\sigma_y = \{0.05, 0.5, 1\}$ from top to down. The Real HRF used for data generation is in green, the estimated FIR average in red, and the estimated IIR average in blue.

estimation which is more realistic than considering space invariant HRF's.

The observations are modeled by the additive white Gaussian noise (AWGN) model and the stimulus activation indicators are modeled by binary variables that are estimated. The prior associated with the binary indicators is a bimodal Gaussian distribution around the 0 and 1 values to cope with the uncertainty related with the noise. The HRF is adaptively estimated under the constraint that it belongs to IIR PBH model [5] space.

Monte Carlo tests using synthetic-1D-block-designed data are performed and the probability of error, P_e, is computed for different noise levels. These tests have shown small P_e, less than the ones obtained with the traditional SPM-GLM [8]. Finally, the average HRF estimation results showed a robust-to-noise close similarity between the real synthetic data HRF and the estimated HRF.

VI. REFERENCES

[1] S. Ogawa, R. S. Menon, D. W. Tank, S. G. Kim, H. Merkle, J. M. Ellermann, and K. Ugurbil, "Functional brain mapping by blood oxygenation level-dependent contrast magnetic resonance imaging. A comparison of signal characteristics with a biophysical model," *Biophys J*, vol. 64, no. 3, pp. 803–812, Mar 1993.

[2] P. Jezzard, P. M. Matthews, and S. M. Smith, *Functional magnetic resonance imaging: An introduction to methods.* Oxford Medical Publications, 2006.

[3] K. J. Friston, "Analyzing brain images: Principles and overview," in *Human Brain Function*. Academic Press USA, 1997, pp. 25–41.

[4] R. B. Buxton, E. C. Wong, and L. R. Frank, "Dynamics of blood flow and oxygenation changes during brain activation: the balloon model," *Magn Reson Med*, vol. 39, no. 6, pp. 855–864, Jun 1998.

[5] D. M. Afonso, J. Sanches, and M. H. Lauterbach, "Neural physiological modeling towards a hemodynamic response function for fMRI," Aug 2007, pp. 1615–1618.

[6] M. H. Hayes, *Statistical Digital Signal Processing and Modeling*. Wiley, March 1996.

[7] John L. Shanks, "Recursion filters for digital processing," *Geophysics*, vol. 32, pp. 33–51, 1967.

[8] J. Sanches, D. Afonso, K. Bartnykas, and M. Lauterbach, "Internal report: Robust bayesian brain activity detection in fmri," Out 2007.